Quantifying fire-specific smoke severity

Jeff Wen[1,*], Patrick Baylis[2], Judson Boomhower[3,4], Marshall Burke[4,5,6]

[1]Department of Earth System Science, Stanford University, Stanford, CA 94305
[2]Department of Economics, University of British Columbia, Vancouver, British Columbia V6T 1Z4, Canada
[3]Department of Economics, University of California, San Diego, La Jolla, CA 92093
[4]National Bureau of Economic Research, Cambridge, MA 02138
[5]Doerr School of Sustainability, Stanford University, Stanford, CA 94305
[6]Center on Food Security and the Environment, Stanford University, Stanford, CA 94305
[*]Corresponding author: jlwen@stanford.edu

Abstract

Rapidly changing wildfire regimes across the Western US has driven more frequent and severe wildfires, resulting in wide-ranging societal threats from the wildfires themselves and the smoke that they generate. However, common measures of fire severity focus on what is burned and do not account for the societal impacts of the smoke generated from each fire. We combine satellite-derived fire scars, air parcel trajectories from individual fires, and predicted smoke $PM_{2.5}$ to link source fires to resulting smoke $PM_{2.5}$ experienced by populations in the contiguous United States from April 2006-2020. We develop a new metric of fire-specific severity based on the cumulative population exposed to smoke $PM_{2.5}$ over the duration of a fire. This measure is only weakly correlated with common measures of wildfire severity, including burned area, structures destroyed, and suppression cost. We find that while recent California fires contributed nearly half of the country's experienced smoke severity during our study period, the most severe individual fire was the 2007 Bugaboo fire in the Southeast. We estimate that a majority of experienced smoke $PM_{2.5}$ comes from sources outside the local jurisdictions where the smoke is experienced, with 87% coming from fires in other counties and 60% from fires in other states. Our approach enables broad-scale assessment of whether specific fire characteristics affect smoke toxicity or impact, informs assessment of the cost-effectiveness of how suppression resources are allocated, and helps clarify the growing transboundary nature of local air quality.

The paper is a non-peer reviewed preprint submitted to EarthArXiv. It has been submitted for publication in a peer reviewed journal, but has yet to be formally accepted for publication.

Introduction

Wildfire regimes have changed in recent decades due to a combination of climate change and a century of fire suppression, and this increase has driven a greater frequency of large wildfire events that result in physical and health related damages from the fine particulate matter ($PM_{2.5}$) in smoke.[1–4] While total $PM_{2.5}$ has been improving in the decades since the Clean Air Act, recent evidence suggests that wildfire smoke $PM_{2.5}$ has begun to reverse this trend, especially in the Western United States.[5–7] This reversal is concerning as recent research suggests that $PM_{2.5}$ from wildfire smoke could be more toxic than $PM_{2.5}$ from other sources,[4] and that existing air quality regulation is poorly equipped to regulate smoke from wildfires.[7] Smoke $PM_{2.5}$ concentrations have now been well measured at broad temporal and spatial scales in the US,[6] and increasing concentrations have been linked to an array of negative societal outcomes, including premature deaths,[8] preterm births,[9] and lower test performance in school-aged children,[10] underscoring the growing social costs of wildfire smoke $PM_{2.5}$ exposure.

Despite growing knowledge of the broad-reaching negative impacts of wildfire smoke exposure, commonly-used metrics of wildfire severity currently do not reflect the societal harm from smoke. Instead, severity metrics typically focus on the number of structures burned, lives tragically lost in the fire itself, the cost of firefighting, and/or total burned area, with the latter a particularly problematic measure given the agreed-upon need for more low-intensity fire (such as prescribed fire) in order to reduce the likelihood of more extreme fires.[11–13]

An inability to link specific fires to their smoke impacts is problematic for at least three reasons. First, the health and societal impacts of smoke from specific fires are plausibly a large proportion of their damage, and the lack of information about the magnitude of these damages hampers efforts to understand whether taxpayer-funded wildfire suppression efforts[14,15] are being allocated to the most damaging fires. Fires that burn structures could produce substantially less smoke than remote fires that send smoke into populated regions. Second, it is increasingly hypothesized that the same amount of smoke from different fires need not have equivalent damages, given that some fires (for example) incinerate chemicals in buildings or burn and aerosolize metals or fungi found in specific soils.[16–18] But these hypotheses remain hard to test on a large scale absent a method to link specific smoke exposures to source fire characteristics. Third, linking smoke exposures to their source fires is important for understanding the transboundary nature of wildfire smoke, and in turn for designing strategies and policies to mitigate smoke exposures. If smoke exposures tend to originate from source fires that are outside county or state jurisdictions where the exposure occurs, as research increasingly suggests,[19–21] then the historic approach of air quality regulation of relying on local jurisdictions to manage exposures by managing local emissions will not be practicable. Jurisdictions are increasingly submitting exceptional event applications to flag and omit air quality exceedances from events such as wildfires,[22] and although these allowances help the jurisdictions remain in attainment of the National Ambient Air Quality Standards, the growth in their use means that transboundary wildfire air pollution issues are basically ignored and residents are unprotected from this important pollution source.

Here, we combine high-resolution estimates of daily smoke $\mathrm{PM}_{2.5}$[6] with a physical model of fire-specific air parcel trajectories to develop a new method for linking specific source fires to the smoke $\mathrm{PM}_{2.5}$ generated by that fire. Our method uses the inverse distance weighted sum of simulated smoke trajectory points to proportionally attribute the daily smoke $\mathrm{PM}_{2.5}$ for each 10km gridcell-day to specific smoke producing fires. This allows us to estimate the share of smoke that each fire has plausibly contributed to downwind locations. We then use this method to derive a novel wildfire smoke $\mathrm{PM}_{2.5}$ severity metric based on the cumulative concentration of smoke $\mathrm{PM}_{2.5}$ that populations experience from each fire, for all identified smoke producing fires between April 2006 and December 2020 (Methods). This metric aggregates the μg/m^3 of smoke $\mathrm{PM}_{2.5}$ experienced by the affected population over the duration of exposure to a specific fire.

The accumulated smoke severity metric allows us to quantify and rank the smoke $\mathrm{PM}_{2.5}$ impacts of individual fires, accounting for the severity, duration, and number of people exposed. This metric does not quantify the health-related impacts from the exposure, but rather provides estimates of the smoke $\mathrm{PM}_{2.5}$ exposure from specific fires at a 10km resolution across the US. We then compare this smoke severity metric to other commonly used wildfire severity and suppression effort metrics such as burned area, suppression cost, and structures burned. Finally, we use our linked estimates to quantify changing patterns and magnitudes of transboundary smoke $\mathrm{PM}_{2.5}$ movement, quantifying how the regional sources of smoke exposure have changed between an earlier, less smokey 2006-2010 period versus a later more smokey 2016-2020 period. We also combine the fire-smoke linked data with estimates of total $\mathrm{PM}_{2.5}$ for 11 Western states[23] to quantify the proportion of total $\mathrm{PM}_{2.5}$ from out-of-county source fires – a quantity relevant to discussions of how to manage local air quality.

Results

Our method of linking source fires to smoke exposure is shown in Figure 1, using a particularly active fire period in CA in 2018 as an example. During this period, three large active fires generated smoke that covered much of California, and this smoke was readily apparent in satellite imagery, recorded in analyst-delineated smoke plumes,[24] and identified in gridded smoke $PM_{2.5}$ data[6] (Figure 1A-1C). We associated daily analyst estimates of smoke-producing fire locations with fire extent polygons and ran forward trajectories of smoke particles emitted at each fire location (Figure 1D). Trajectories were then used to partition the contribution of each source fire to estimated wildfire smoke $PM_{2.5}$ (Figure 1E, Methods), and fire-specific smoke severity calculated as the sum of population exposed to each μg/m^3 of smoke on each day for the duration of each fire (Supplemental Figure S1). Validation of our approach on days in which only one fire was burning shows that our approach captures nearly all of the smoke emitted by a given fire and aligns closely with visible satellite imagery on the same day, though we note that satellite resolution constraints can lead to conservative estimates of contributed smoke $PM_{2.5}$ in some cases (Methods, Supplemental Figure S2-S3). On days in which multiple fires are burning and locations experience overlapping smoke from multiple fires, fire-specific attributions are less certain, and we thus compute a fire-specific "attribution certainty score" that calculates the percent of a fire's overall attributed severity that occurs on days when smoke from other fires is not present (Methods, Supplemental Figure S4); more isolated fires have attributed severities that are more certain.

We rank the top fires by accumulated smoke severity and show the top 9 fires in Figure 2 and the top 20 fires in Supplemental Table S1. Out of the top 9, 6 of the fires are from the 2020 fire season and 7 of these top fires originated in California. Perhaps surprisingly, the Bugaboo fire, which originated in Georgia in 2007 and is the only top fire that originated on the East coast, is ranked as the most severe fire by our accumulated smoke severity metric, nearly twice as severe as the next most severe fire. This fire spread dense smoke across highly populated areas of the US Southeast for over a month (Supplemental Figure S5). The four other fires in the top 5 most severe fires were all in California. Three of these fires – August Complex, Dolan, and Bobcat, all in 2020 – were in late summer, a period during which prevailing winds carried smoke across much of the US West and Midwest for weeks. The fourth, the 2018 Camp Fire, was during late fall, where easterly winds blew thick smoke into highly-populated CA regions for a short period. On a population-weighted basis, we calculate that the Camp Fire generated the densest smoke of the fires in our sample, with the Bugaboo Fire second (Supplemental Table S1). Other fires in the top ten tended to be late summer fires on the West Coast (CA, OR), where large amounts of smoke were again blown east across much of the US West and Midwest.

We compare our accumulated smoke severity metric with different commonly used wildfire severity and suppression effort metrics, including burned area, structures burned,[25] and fire suppression cost.[26] Smoke severity is positively but weakly correlated with burned area, one of the most commonly used measures of fire activity and severity. We estimate that variation in log burned area between fires only explains about 12% of the variation in log smoke severity (Figure 3A). While there are few very large fires with low smoke severity, we see a substantial number of relatively small fires with high smoke severity, indicating that the specific location and timing of fire starts can exert large influence over the population exposed to a fire's smoke. We see similarly positive but weak relationships between our smoke severity measure and expenditures on fire suppression (Figure 3B) and counts of structures destroyed in each fire (Figure 3C). Regarding fire suppression, while the most smoke-severe fires were those that tended to receive the most suppression resources (upper right corner of Figure 3B), we document a substantial number of fires where smoke severity was high but suppression efforts modest (points in upper left), and a similarly high number where suppression costs were high but smoke impacts modest (lower right). Consistent with this relationship and with the recent finding that fire suppression costs are overwhelmingly determined by the threat of fires to physical structures,[26] we find that smoke severity only weakly tracked structure damage.

We use our linked fire-smoke estimates to quantify the changing overall burden of smoke exposure, to locate the main sources of this exposure, and to characterize the transboundary nature of overall exposure. The magnitude of smoke $PM_{2.5}$ that the US population experienced doubled from the early less smokey period in 2006-2010 to the more smokey late period in 2016-2020 (Figure 4A). California was by far the largest source and recipient of wildfire smoke in both periods, with the contribution of CA-sourced smoke to total smoke severity growing from 26% in the early period to 40% in the late period. While multiple states in the Midwest, South, and East were in the top-5 smoke recipients prior to 2010, a ranking driven in part by large populations in those states, the recent rapid increase in fire activity in the West has meant that Western states now bear a much larger share of the accumulated smoke exposure, sourced from themselves or nearby states.

On average across the US over our study period, we calculate that nearly 93% of the experienced smoke severity came from "trans-county" sources (i.e. source fires outside the county where the smoke was experienced) and 62% from trans-state sources. In many states, a large portion of smoke $PM_{2.5}$ remains within state borders, but Western US states, such as California, Idaho, and Montana, contribute large amounts of smoke $PM_{2.5}$ to neighboring states (Supplemental Figure S6). For recipients of this smoke, large percentages of smoke exposure (e.g. 94% in Nevada) come from out-of-state. Regarding international smoke transport, we find that the share of overall smoke severity experienced in the US attributable to fires in Canada and Mexico has held steady in both periods at around 8% and 3%, respectively, suggesting that a large proportion (nearly 90%) of experienced smoke severity in the US comes from domestic fires.

Using independent gridded estimates of total $PM_{2.5}$,[23] we quantify the contribution of transboundary wildfire smoke $PM_{2.5}$ to total $PM_{2.5}$ between the early (2006-2010) and late (2016-2020) periods. We find that all counties in the Western US (414 counties) experienced an increase in the proportion of total $PM_{2.5}$ from out-of-county fire sources (Figure 4B). This finding aligns with recent literature suggesting a reversal of trends in overall air pollution due to wildfire smoke[7,27,28] and links these reversals to transboundary out-of-county fire sources. In the later period, we calculate that for 120 counties, over a quarter of the total $PM_{2.5}$ in that county was from trans-county smoke sources (there were no such counties in the early period) and in 3 counties, over half of total $PM_{2.5}$ was from trans-county sources.

Discussion

Our study develops a new method for measuring wildfire severity by connecting individual wildfires to the smoke $PM_{2.5}$ experienced by populations downwind of each fire. Using our smoke severity metric, we find that many of the most severe wildfires are from the recent 2020 California wildfire season, other fire severity and suppression effort metrics are only moderately correlated with the smoke severity measure, and that the transboundary share of wildfire smoke has been increasing in recent years and is a substantial contributor to total $PM_{2.5}$ concentrations in many counties in the West.

Compared to existing efforts that aim to link smoke to fire sources, our method provides granular fire-specific attribution of smoke $PM_{2.5}$ and estimates of impacts across the contiguous US at a 10km spatial resolution from April 2006 to December 2020. Existing literature has used the HYSPLIT model[19] to understand smoke transport, but focused on regional transport of smoke rather than specific fire transport and also did not quantify the attributed smoke $PM_{2.5}$. Recent research has used other simplified Lagrangian particle transport models[29] to produce back trajectories of simulated air parcels arriving at specific locations and provide estimates of $PM_{2.5}$ from wildfire smoke. However, this analysis focused on summer months and only conducted population smoke $PM_{2.5}$ analysis for 33 population centers, as compared to our analysis which extends beyond the summer months and covers the contiguous US. The relatively coarse resolution of these analyses' source regions make it challenging to consider the impact from specific fires.

Other researchers have used a combination of chemical transport models (CTMs),[30] simplified transport models,[31] and close proximity air pollution monitors[32] to study the impact of wildfires on ambient air quality. However, these studies have primarily only considered the impact of active fires on a relatively small spatial area and the analyses do not cover multiple fires and years. In our work, we consider all smoke-producing fires identified by satellite imagery and trained analysts[6] from April 2006-2020. Although CTMs are commonly used to estimate the impact of specific air pollutants on downwind communities,[33–35] uncertainty around surface fuel characteristics and emission inventories result in highly variable estimates of particulate matter air pollution from fires.[36,37] Additionally, the computational burden of running these models limits their applicability in our context, as comprehensive characterization of smoke contributions would require a separate model run for each of the fires in our data. Related studies that use satellite imagery or surface observations to analyze air pollution trends in the Western US[6,38–40] provide insight into the overall contribution of wildfire to regional air quality trends but are unable to link smoke to specific source fires.

Our smoke-linking method provides a conservative estimate of the smoke $PM_{2.5}$ contributed by specific fires, as shown by analysis of isolated fires where our method captures most but not all of nearby smoke (Supplemental Figure S2-S3). Attributions are limited in part by analysts' abilities to identify smoke-producing fire points, from which HYSPLIT trajectories are initialized, and our ability to accurately match fire points to fire polygons. Future work that leverages satellite sensors with higher spatial and temporal resolution could improve the identification of smoke producing fires and/or active fire burned areas and refine the fire ignition point to fire polygon match. Improved estimates of plume injection heights could also improve estimates, as literature suggests that the injection height of smoke plumes play a large role in smoke transport but that accurate estimates of fire-specific injection heights are limited.[37] To account for uncertainty in the injection height of plumes, we initialize trajectories at 3 different injection heights for each fire (Methods), and future improvements that incorporate satellite observed or modeled plume injection heights could result in more accurate trajectories.[41]

Our smoke severity metric assumes that severity is a linear function of accumulated daily exposure, and that populations in different locations respond similarly to accumulated exposure. We believe this linearity assumption is broadly consistent with the pollution-health literature, which has recently described all-source $PM_{2.5}$ mortality concentration-response functions that are roughly linear at both low and high concentrations of particulate exposure,[42,43] and wildfire-specific mortality concentration-response functions that are similarly linear in smoke $PM_{2.5}$.[44] In the absence of additional evidence on whether response functions differ across locations, we follow this literature and assume linear impacts, which allows straightforward aggregation of severity using the sum of contributed smoke $PM_{2.5}$ that populations experience from specific fires. Our approach could account for nonlinear mappings of exposure to severity, or heterogeneous impacts by location, if future data support such revisions.

Our analysis identifies the Bugaboo Scrub Fire in 2007 as producing the highest smoke severity during our study period. One potential reason for the high impact of this fire is its proximity to large urban areas and that smoke from this fire transported across much of the Eastern Seaboard (Supplemental Figure S5). Recent research also suggests that slower burning smouldering fires, similar to the peatland fires in the Bugaboo fire, could release large amounts of harmful particulate matter due to incomplete combustion of surface matter, which ultimately results in high smoke $PM_{2.5}$ emissions.[37,45] Better understanding the landscape features that predict smoke severity is an active and important area for additional work. While the Bugaboo fire could have truly been more smoke-producing than other fires, we note that the fire had a higher attribution certainty (score of 89%) compared to other top fires, such as the 2020 California fires (attribution certainty scores around 50%) suggesting greater uncertainty around the smoke severity of the 2020 California fires because multiple other fires were occurring at the same time and contributing smoke to the same locations (Supplemental Table S1).

The weak correlation between our smoke severity metric and other common measures of fire severity is consistent with the large observed share of suppression resources spent on limiting physical property damage.[26,46] Fires close to urban areas threaten structures (and, in a direct way, lives) and receive more suppression effort, but often expose much smaller populations to smoke; fires further from populated areas threaten fewer structures and receive less suppression effort, but can generate large amounts of smoke that have more indirect but likely very large health impacts, including increased mortality. Further recognition and quantification of these downwind impacts may help inform and shift future resource allocation decisions.[12]

Our method links smoke $PM_{2.5}$ to source fires, which enables further analysis to better understand the drivers of differential smoke toxicity. Recent literature suggests that wildfires can convert and release toxic elements, such as hexavalent chromium, into the atmosphere, but analysis has been limited to specific study sites.[47] This work provides an approach to investigate these findings at a broader-scale and also enables further research into whether burning specific materials, such as man-made structures, results in more toxic air pollution.[48]

As the climate continues to warm and wildfires increase across much of the Western US and beyond,[1,49] particulate matter air pollution from these events is trending upward and expected to worsen in the coming decades.[5–7,50] A growing literature finds that exposure to wildfire smoke results in a range of negative societal impacts, including impacts on respiratory-related morbidity and all-cause mortality,[44,51,52] interrupted learning,[10,53] and decreased labor productivity.[54] Our work provides a method to connect these smoke $PM_{2.5}$ impacts back to specific source fires, and can help clarify policy options that aim to better allocate resources to address this growing environmental challenge.

Methods

HYSPLIT trajectories for smoke-producing fires In this work, we leverage the Hybrid Single-Particle Lagrangian Integrated Trajectory (HYSPLIT) model[55] to track the movement of smoke emitted from particular fires and to allocate $PM_{2.5}$ surfaces back to source fires. These data represent simulated forward trajectories of smoke particles emitted at smoke-producing fire points (HYSPLIT points) for all automatically detected and manually added fire hotspots identified by trained Hazard Mapping System (HMS) analysts[19,56] between April 2006 and December 2020. The satellite-detected fire points are validated and identified as smoke-producing by HMS analysts and false positives are removed to generate a set of HYSPLIT initialization points, from which forward trajectories are run (see supplemental information of Childs et al. (2022)[6] for details of trajectory generation). To incorporate uncertainty about smoke injection heights, we initialize three trajectories at each point beginning at different altitudes (500, 1500, and 2500 meters above ground level).

In total, there are 2.4 million distinct HYSPLIT points from April 2006 - December 2020 that each have three associated 6-day trajectories (one for each initial altitude). Each trajectory is defined as a sequence of estimated latitude, longitude, and height coordinates at hourly time steps following initialization. For each trajectory, we calculate the cumulative rainfall and minimum height so far on the trajectory path. We truncate each trajectory path by removing trajectory points that have been rained out or that have collided with the ground. With the remaining trajectory points, we calculate the cumulative trajectory distance from the fire polygon centroid or initial HYSPLIT point (if the initialization point did not fall within any fire polygons) to each successive point on the trajectory path, which we later use to distribute smoke $PM_{2.5}$. For each HYSPLIT point, HMS analysts assign a ”duration” value that represents the number of hours that the specific fire produces smoke and analysts may duplicate fire points to represent severe smoke producing fires. We run trajectories over the duration of each fire and remove duplicated fire points to reduce computation. After generating fire trajectories, we weigh each initialization point to account for the duplicated fire points that had been identified for that initialization time.

Assigning HYSPLIT initialization points to fires To group HYSPLIT points, which are not associated with specific named fires, belonging to the same source fire, we match the location of HYSPLIT points to a separate database of known fires. We use fire boundary shapes from the GlobFire v3 dataset subsetted to North America from April 2006-2020.[57] These fire polygons represent the final area of fires detected by NASA's Moderate-Resolution Imaging Spectroradiometer (MODIS) satellite and provide a single polygon of the total burned area for each detected fire with start and end dates. After matching the fire polygons with the locations of the smoke-producing HYSPLIT points, we filter for points that fall between the initial date and end date of the fire polygons. The resulting matched dataset represents the fire polygons and associated smoke-producing fire points.

Because a large number of HYSPLIT points are satellite derived, the accuracy of the fire location is dependent on the resolution of the satellite product used to identify these fires and recent literature has suggested that the accuracy of HYSPLIT points is around 2-3km.[19] As shown in Supplemental Figure S7, the HYSPLIT points, which are partially algorithmically identified as thermal hotspots, appear to follow a rectangular grid and result in some smoke producing HYSPLIT points that fall outside of the buffered fire polygon. These points likely belong to the fire as there are no other fires nearby at this time and could contribute to decreased attribution of contributed smoke $PM_{2.5}$ to this specific fire. Aligned with recent research that has shown a 2km median spatial offset between the MODIS burned area product and identified fire points,[58] we add a 2km buffer to the boundary of detected fire polygons to account for this potential resolution-based inaccuracy. A larger buffer around the fire polygon would lead to more associated HYSPLIT points per fire and therefore potentially larger smoke severity estimates, at the potential cost of associating HYSPLIT points with the wrong fire. We take the conservative approach and use a 2km buffer, as suggested by the literature.

About 65% (1546271/2372751) of the nearly 2.4 million HYSPLIT points (smoke-producing fires) are matched to a fire polygon with a majority of the unmatched HYSPLIT points occurring in recent years (Supplemental Figure S8). One potential reason for more unmatched fire points in recent years is the inclusion of the hotspot detections from the Visible Infrared Imaging Radiometer Suite (VIIRS) sensor starting in 2016, which has a higher resolution and detects more thermal anomalies[59] than previous thermal sensors used by the HMS system. To ensure that we do not ignore the smoke generated from the unmatched HYSPLIT points, we assume that if a HYSPLIT point does not fall into a buffered fire polygon, then it is a separate fire.

Calculating smoke $PM_{2.5}$ from specific fires To estimate the contribution of smoke $PM_{2.5}$ from specific fires, we combine the fire polygon matched trajectories with previous estimates of daily 10-kilometer (km) smoke $PM_{2.5}$ over the period from April 2006-2020.[6] We first match trajectory points to 10km gridcells using the trajectories described above for all of North America from April 2006-2020.

After linking trajectory points (and initial source fire) to overlapping gridcells, we use a window function (spatial buffer) to account for the spatial dispersion of smoke particulates, as trajectory points represent a single point estimate of the likely location that an air parcel traveled. In reality, the air pollution from smoke could disperse and affect a larger area. We considered different window sizes ranging from no buffering around the gridcell where a trajectory point landed (just consider the 10km gridcell where a trajectory point landed), all immediately neighboring gridcells (effectively a 30km window centered on the gridcell where a trajectory point landed), and two rings of neighboring 10km gridcells (a 50km window centered on the gridcell where the trajectory point landed). We find that the 10km window potentially underestimates the amount of smoke $PM_{2.5}$ leaving on average over 60% of smoke $PM_{2.5}$ unaccounted for (Supplemental Figure S9). We conduct the analysis with the 30km window, which is more conservative than the 50km window but makes up for a large portion of the smoke $PM_{2.5}$ that the 10km window misses.

To distribute smoke $PM_{2.5}$ at the gridcell to individual fires, we consider the number of trajectory points and cumulative trajectory distance of those points from a source fire. Specifically, as shown in Supplemental Figure S1, for an individual gridcell, we first calculate the denominator total gridcell weight as the sum of inverse distance weighted trajectory point counts. In the supplemental figure example of the multiple fire, there are 5 trajectory points in gridcell 3 with 2 belonging to fire A and 3 belonging to fire B. Each of these trajectory points has a cumulative trajectory distance. The total gridcell weight is the sum of these inverse cumulative trajectory distances. This simplified example does not consider the spatial buffer described above, but the 30km spatial buffer used in the main analysis would work similarly and also count trajectory points in the neighboring ring of gridcells. After calculating this total gridcell weight, we calculate a fire-specific gridcell share, which sums the inverse distance weighted trajectory counts from a specific fire and normalizes the value by the total gridcell weight. In Supplemental Figure S1, fire A is calculated to have 10% share of smoke $PM_{2.5}$ in gridcell 3 and fire B accounts for the remaining 90% share of smoke $PM_{2.5}$. The calculation of smoke $PM_{2.5}$ from a single fire is the same as in the multiple fire case; however, because there are no trajectory points from other fires the calculated share for the single fire is 100%. Lastly, to distribute the smoke $PM_{2.5}$ in a specific gridcell to individual fires, we multiply the share with the total smoke $PM_{2.5}$ in the gridcell.

Estimating population smoke severity in each gridcell We estimate the population impacted by smoke $PM_{2.5}$ from specific fires by combining the wildfire attributed smoke $PM_{2.5}$ with gridded population data from WorldPop.[60] We use the unconstrained individual countries 2000-2020 UN adjusted (1km resolution) dataset (`https://hub.worldpop.org/doi/10.5258/SOTON/WP00671`) and download data for the US. We first calculate the yearly population in 10km gridcells aligning with our smoke $PM_{2.5}$ grid by taking an area-weighted sum of the 1km WorldPop grid cells that fall into our 10km smoke $PM_{2.5}$ grid across the contiguous US from 2006-2020. Then to calculate the daily smoke severity at the gridcell, we multiply the fire-specific contributed smoke $PM_{2.5}$ with the population at the gridcell. In Supplemental Figure S1, for the multiple fire case, gridcell 3 has a population of 10 so the smoke severity from fire A is the product of fire A's share, the total smoke $PM_{2.5}$, and the population in the gridcell, which equals 20 person μg/m^3. Smoke severity for fire B follows a similar calculation and is estimated to have 180 person μg/m^3 smoke severity. To calculate the smoke severity for an individual fire over the duration of the fire, we sum the daily smoke severity across gridcells and days.

Comparison with fire suppression costs and structures burned To estimate the relationship between suppression costs and population-weighted smoke $PM_{2.5}$ exposure, we use data from Baylis and Boomhower (2019),[26] which includes fire suppression costs for fires in 11 Western states from 2006-2016. Due to lack of consistent fire suppression cost reporting, we focus analysis on fires larger than 300 acres. The fire fighting suppression costs are collected from different Freedom of Information Act and public records requests to six federal and state agencies. We direct interested readers to Baylis and Boomhower (2019)[26] for additional details. We match the fire suppression cost data to specific fires by identifying observations that fall into buffered (500m) fire polygons and by ensuring that the ignition date present in the suppression dataset falls within 2 days of the initial start date of the fire polygon. We match the destroyed structures dataset[25] to individual fires in a similar way by filtering to the matching year and finding structure burned locations that fall within the buffered fire polygons.

Calculating total $PM_{2.5}$ for transboundary analysis In order to compare smoke $PM_{2.5}$ to total $PM_{2.5}$ for counties, we calculate the average daily total $PM_{2.5}$ for each 10km gridcell in 11 Western States from 2006-2020 using data from Swanson et al. (2022).[23] We use the `exactextractr` R package and take the area weighted mean of the 1km gridcells that fall into the smoke $PM_{2.5}$ 10km gridcells. We then identify the 10km gridcells that overlap with counties and sum over the gridcell-days for both smoke $PM_{2.5}$ and total $PM_{2.5}$. Using the location of the source fire and the amount of contributed smoke $PM_{2.5}$ in each gridcell, we can calculate the proportion of total $PM_{2.5}$ in each gridcell that comes from out-of-county source fires.

Calculating attribution certainty score for each fire The fire-specific attribution certainty score estimates the percent of a fire's smoke severity that happens on days when there is no smoke from other fires. To calculate this score, we take a weighted average of the share of gridcell smoke $PM_{2.5}$ weighting by the smoke severity of a specific fire. We walk through an example of this calculation for the single versus multiple fire case in Supplemental Figure S4. As described above, the share calculation of a fire takes into account the number of trajectory points and the cumulative trajectory distance of the points that belong to a specific fire divided by the gridcell total weight.

Code and data availability Data and code to replicate all results in the paper will be made available upon publication.

Acknowledgements We thank Jessica Li for help generating HYSPLIT trajectory data, Kimiko Barrett for sharing data on structures burned, and the ECHOLab at Stanford University for helpful discussions. We also thank Stanford University and the Stanford Research Computing Center for providing computational resources that contributed to these research results. MB thanks the Robert Wood Johnson Foundation (ID# 76555) and the Stanford Woods Institute Environmental Ventures Project for funding. JW gratefully acknowledges funding from Stanford Data Science and The Ram and Vijay Shriram Sustainability Fellowship for this work. JB thanks the Carnegie Corporation of New York. The funders had no role in study design, data collection and analysis, decision to publish or preparation of the manuscript.

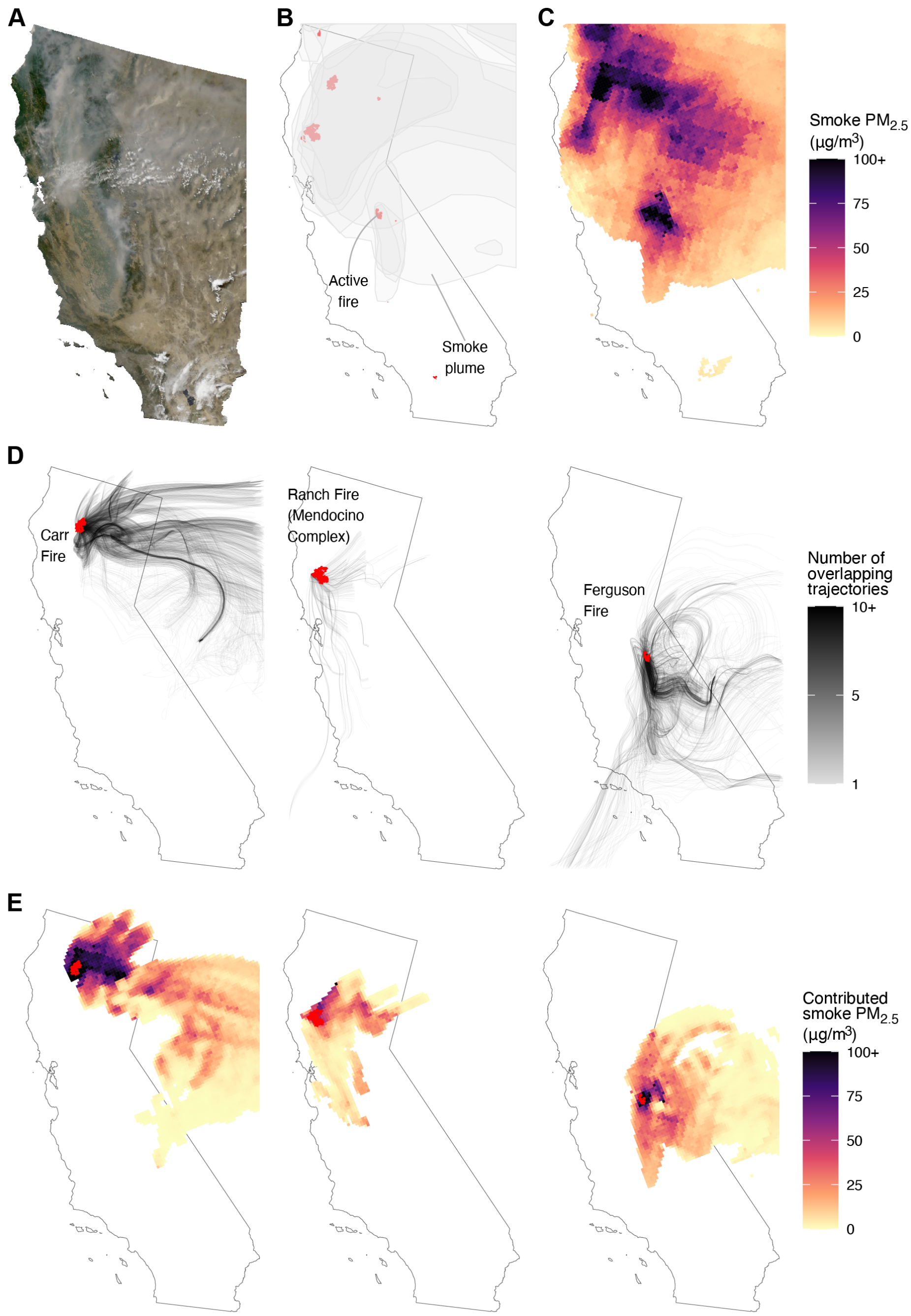

Figure 1: **Attributing wildfire smoke $PM_{2.5}$ to source fires**, using active fires in CA on July 29th, 2018 as an example. **A.** Geostationary satellite imagery over California with visible smoke. **B.** Hazard Mapping System smoke plume annotations shown in gray. Active fires are shown as red polygons. **C.** Wildfire smoke $PM_{2.5}$ from all fires with smoke $PM_{2.5}$ capped at $100\mu g/m^3$, using data from ref.[6] **D.** Hybrid Single-Particle Lagrangian Integrated Trajectory (HYSPLIT) trajectories for three main active fires on July 29th. Each path represents the movement of a particle that originated within the fire polygon up to 5 days before July 29th. Darker paths suggest that more particles followed that trajectory. **E.** July 29th snapshot of the estimated contribution of each fire to smoke $PM_{2.5}$.

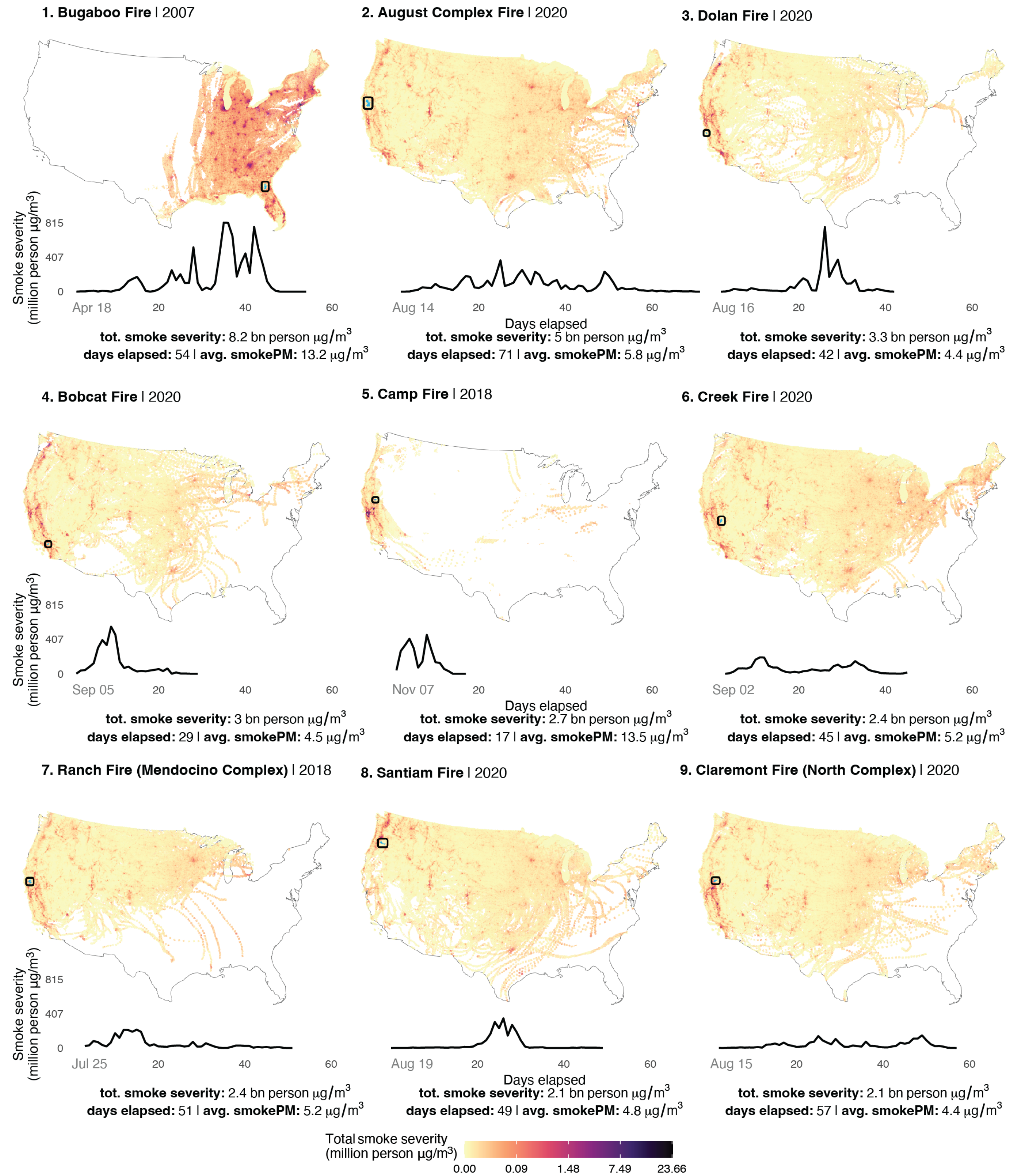

Figure 2: **Top fires by ranked accumulated smoke severity from April 2006-2020.** Each small multiple map shows the total accumulated smoke $PM_{2.5}$ severity aggregated over the duration of the fire. This severity metric considers the amount of smoke $PM_{2.5}$, the population affected, and the total number of days of smoke exposure. The line chart shows the smoke severity over time from the initial day of the fire. Initial fire locations are cyan colored and outlined in black.

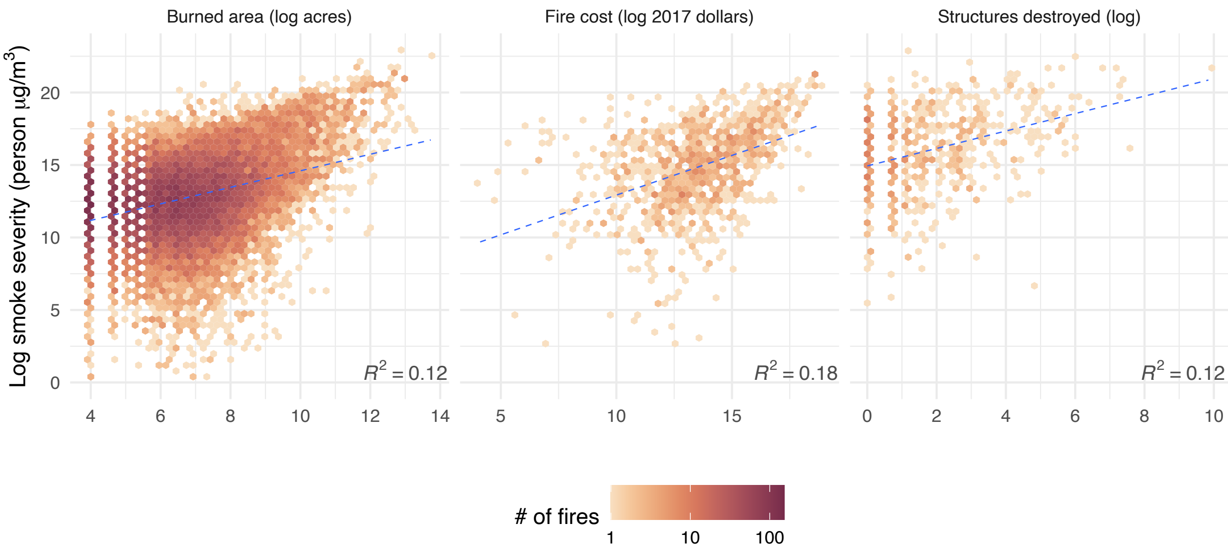

Figure 3: **Comparison between common fire-related metrics and accumulated smoke severity.** From left to right, the panels show the relationship between the natural log of burned area (acres), fire suppression cost (2017 dollars), or structures destroyed (# structures) versus accumulated smoke severity (person μg/m^3) with the color of the hexbin indicating the count of individual fires. In the left plot, the burned area is calculated from the GlobFire dataset for fires from April 2006-2020 ($n = 18,606$). For the center plot, only fires greater than 300 acres burned from April 2006-2016 in the Western US are shown due to inconsistent fire suppression cost data for smaller fires and the limited time frame of the fire cost source dataset ($n = 984$). The right plot shows available data on destroyed structures data for the contiguous US from April 2006-2020 ($n = 558$). The blue dotted lines represent the fitted regression lines.

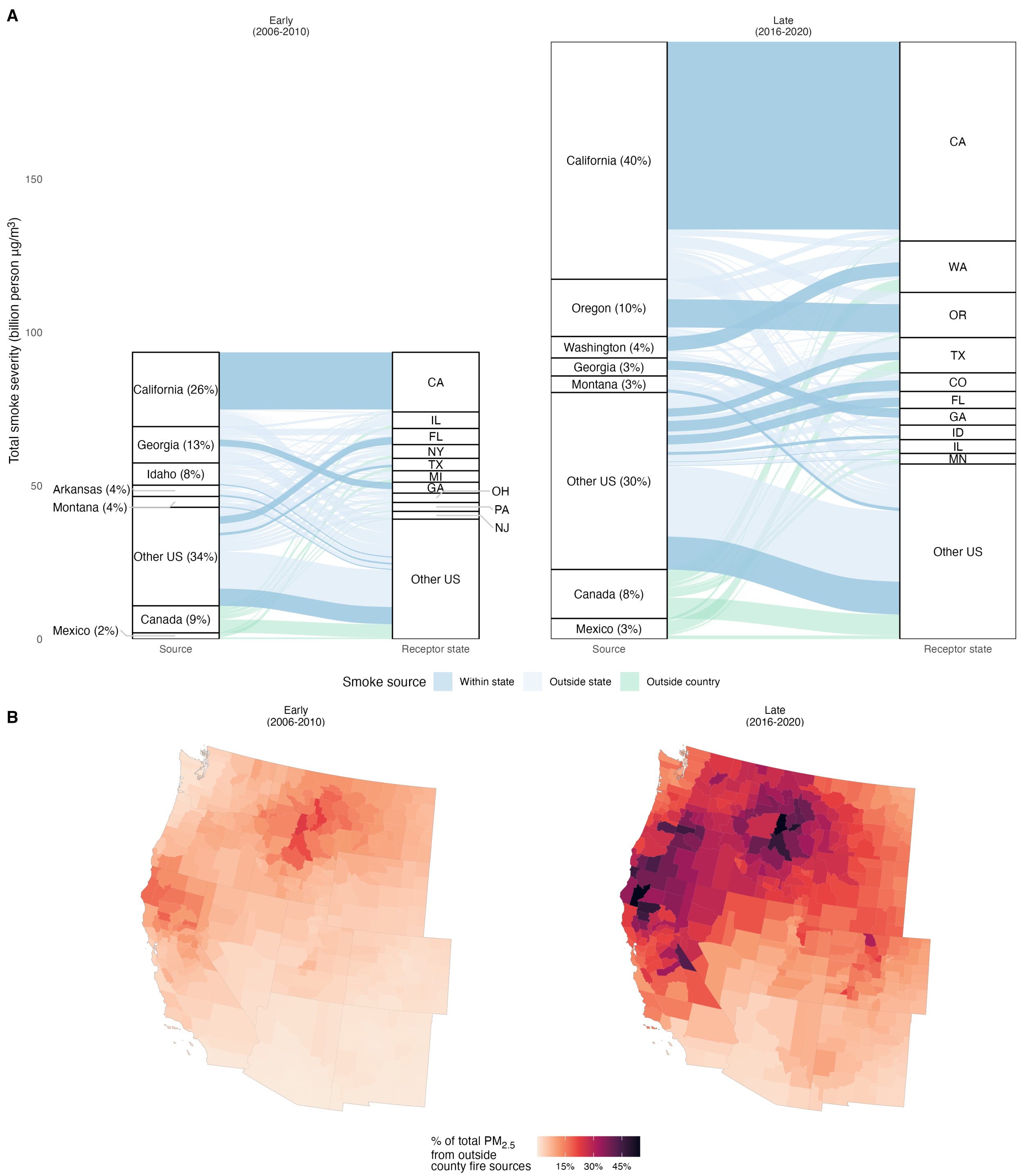

Figure 4: **Trans-state and -county boundary transport of smoke $PM_{2.5}$, and contribution of transboundary smoke to total $PM_{2.5}$ concentrations. A.** Alluvial diagram of smoke $PM_{2.5}$ from source to receptor states in the early (2006-2010) and late (2016-2020) periods. Percentages represent the % of total smoke severity contributed by that state. The dark blue flows represent within state, light blue outside state, and green flows outside country transport of smoke $PM_{2.5}$. **B.** The fraction of total $PM_{2.5}$ from source fires that are outside of the county in the early (2006-2010) and late (2016-2020) periods has grown dramatically especially across the Pacific Northwest, California, Idaho, and Montana.

References

[1] John T Abatzoglou and A Park Williams. Impact of anthropogenic climate change on wildfire across western us forests. *Proceedings of the National Academy of Sciences*, 113(42):11770–11775, 2016.

[2] Bonne Ford, Maria Val Martin, SE Zelasky, EV Fischer, SC Anenberg, Colette L Heald, and JR Pierce. Future fire impacts on smoke concentrations, visibility, and health in the contiguous united states. *GeoHealth*, 2(8):229–247, 2018.

[3] Colleen E Reid and Melissa May Maestas. Wildfire smoke exposure under climate change: impact on respiratory health of affected communities. *Current opinion in pulmonary medicine*, 25(2):179, 2019.

[4] Rosana Aguilera, Thomas Corringham, Alexander Gershunov, and Tarik Benmarhnia. Wildfire smoke impacts respiratory health more than fine particles from other sources: observational evidence from southern california. *Nature communications*, 12(1):1–8, 2021.

[5] Rebecca R Buchholz, Mijeong Park, Helen M Worden, Wenfu Tang, David P Edwards, Benjamin Gaubert, Merritt N Deeter, Thomas Sullivan, Muye Ru, Mian Chin, et al. New seasonal pattern of pollution emerges from changing north american wildfires. *Nature communications*, 13(1):1–9, 2022.

[6] Marissa L Childs, Jessica Li, Jeffrey Wen, Sam Heft-Neal, Anne Driscoll, Sherrie Wang, Carlos F Gould, Minghao Qiu, Jennifer Burney, and Marshall Burke. Daily local-level estimates of ambient wildfire smoke pm2. 5 for the contiguous us. *Environmental Science & Technology*, 2022.

[7] Marshall Burke, Marissa L Childs, Brandon De la Cuesta, Minghao Qiu, Jessica Li, Carlos F Gould, Sam Heft-Neal, and Michael Wara. Wildfire influence on recent us pollution trends. Technical report, National Bureau of Economic Research, 2023.

[8] Christopher JL Murray, Aleksandr Y Aravkin, Peng Zheng, Cristiana Abbafati, Kaja M Abbas, Mohsen Abbasi-Kangevari, Foad Abd-Allah, Ahmed Abdelalim, Mohammad Abdollahi, Ibrahim Abdollahpour, et al. Global burden of 87 risk factors in 204 countries and territories, 1990–2019: a systematic analysis for the global burden of disease study 2019. *The Lancet*, 396(10258):1223–1249, 2020.

[9] Sam Heft-Neal, Anne Driscoll, Wei Yang, Gary Shaw, and Marshall Burke. Associations between wildfire smoke exposure during pregnancy and risk of preterm birth in california. *Environmental Research*, 203:111872, 2022.

[10] Jeff Wen and Marshall Burke. Lower test scores from wildfire smoke exposure. *Nature Sustainability*, pages 1–9, 2022.

[11] Malcolm North, Brandon M Collins, and Scott Stephens. Using fire to increase the scale, benefits, and future maintenance of fuels treatments. *Journal of Forestry*, 110(7):392–401, 2012.

[12] DW Schweizer and R Cisneros. Forest fire policy: change conventional thinking of smoke management to prioritize long-term air quality and public health. *Air Quality, Atmosphere & Health*, 10(1):33–36, 2017.

[13] Paul F Hessburg, Susan J Prichard, R Keala Hagmann, Nicholas A Povak, and Frank K Lake. Wildfire and climate change adaptation of western north american forests: a case for intentional management. *Ecological applications*, 31(8):e02432, 2021.

[14] Malcolm P North, Scott L Stephens, Brandon M Collins, James K Agee, G Aplet, Jerry F Franklin, and Peter Z Fule. Environmental science. reform forest fire management. *Science*, 349(6254):1280–1281, 2015.

[15] Courtney A Schultz, Matthew P Thompson, and Sarah M McCaffrey. Forest service fire management and the elusiveness of change. *Fire ecology*, 15(1):1–15, 2019.

[16] Yong Ho Kim, Sarah H Warren, Ingeborg Kooter, Wanda C Williams, Ingrid J George, Samuel A Vance, Michael D Hays, Mark A Higuchi, Stephen H Gavett, David M DeMarini, et al. Chemistry, lung toxicity and mutagenicity of burn pit smoke-related particulate matter. *Particle and Fibre Toxicology*, 18(1):1–18, 2021.

[17] Leda N Kobziar, Melissa RA Pingree, Heather Larson, Tyler J Dreaden, Shelby Green, and Jason A Smith. Pyroaerobiology: the aerosolization and transport of viable microbial life by wildland fire. *Ecosphere*, 9(11):e02507, 2018.

[18] Leda N Kobziar, David Vuono, Rachel Moore, Brent C Christner, Timothy Dean, Doris Betancourt, Adam C Watts, Johanna Aurell, and Brian Gullett. Wildland fire smoke alters the composition, diversity, and potential atmospheric function of microbial life in the aerobiome. *ISME Communications*, 2(1):1–9, 2022.

[19] Steven J Brey, Mark Ruminski, Samuel A Atwood, and Emily V Fischer. Connecting smoke plumes to sources using hazard mapping system (hms) smoke and fire location data over north america. *Atmospheric Chemistry and Physics*, 18(3):1745–1761, 2018.

[20] Marshall Burke, Anne Driscoll, Sam Heft-Neal, Jiani Xue, Jennifer Burney, and Michael Wara. The changing risk and burden of wildfire in the united states. *Proceedings of the National Academy of Sciences*, 118(2), 2021.

[21] Katelyn O'Dell, Kelsey Bilsback, Bonne Ford, Sheena E Martenies, Sheryl Magzamen, Emily V Fischer, and Jeffrey R Pierce. Estimated mortality and morbidity attributable to smoke plumes in the united states: Not just a western us problem. *GeoHealth*, 5(9):e2021GH000457, 2021.

[22] Liji M David, AR Ravishankara, Steven J Brey, Emily V Fischer, John Volckens, and Sonia Kreidenweis. Could the exception become the rule¿uncontrollable'air pollution events in the us due to wildland fires. *Environmental Research Letters*, 16(3):034029, 2021.

[23] Alan Swanson, Zachary A Holden, Jon Graham, D Allen Warren, Curtis Noonan, and Erin Landguth. Daily 1 km terrain resolving maps of surface fine particulate matter for the western united states 2003–2021. *Scientific Data*, 9(1):1–13, 2022.

[24] National Oceanic and Atmospheric Administration. Hazard mapping system fire and smoke product. `https://www.ospo.noaa.gov/Products/land/hms.html#about`.

[25] National Fire and Aviation Management (FAMWEB) and National Interagency Fire Center (NIFC), as reported by Headwaters Economics. Wildfires destroy thousands of structures each year. Technical report, Headwaters Economics, 2022. `https://headwaterseconomics.org/natural-hazards/structures-destroyed-by-wildfire`.

[26] Patrick Baylis and Judson Boomhower. The economic incidence of wildfire suppression in the united states. *American Economic Journal: Applied Economics*, 15(1):442–73, January 2023.

[27] Michael Jerrett, Amir S Jina, and Miriam E Marlier. Up in smoke: California's greenhouse gas reductions could be wiped out by 2020 wildfires. *Environmental Pollution*, 310:119888, 2022.

[28] TY Wilmot, AG Hallar, JC Lin, and DV Mallia. Expanding number of western us urban centers face declining summertime air quality due to enhanced wildland fire activity. *Environmental Research Letters*, 16(5):054036, 2021.

[29] Taylor Y Wilmot, Derek V Mallia, A Gannet Hallar, and John C Lin. Wildfire activity is driving summertime air quality degradation across the western us: a model-based attribution to smoke source regions. *Environmental Research Letters*, 17(11):114014, 2022.

[30] Hongrong Shi, Zhe Jiang, Bin Zhao, Zhijin Li, Yang Chen, Yu Gu, Jonathan H Jiang, Meemong Lee, Kuo-Nan Liou, Jessica L Neu, et al. Modeling study of the air quality impact of record-breaking southern california wildfires in december 2017. *Journal of Geophysical Research: Atmospheres*, 124(12):6554–6570, 2019.

[31] Uwayemi Sofowote and Frank Dempsey. Impacts of forest fires on ambient near–real–time pm2.5 in ontario, canada: Meteorological analyses and source apportionment of the july 2011–2013 episodes. *Atmospheric Pollution Research*, 6(1):1–10, 2015.

[32] Shekar Viswanathan, Luis Eria, Nimal Diunugala, Jeffrey Johnson, and Christopher McClean. An analysis of effects of san diego wildfire on ambient air quality. *Journal of the Air & Waste Management Association*, 56(1):56–67, 2006.

[33] Rodrigo Munoz-Alpizar, Radenko Pavlovic, Michael D Moran, Jack Chen, Sylvie Gravel, Sarah B Henderson, Sylvain Ménard, Jacinthe Racine, Annie Duhamel, Samuel Gilbert, et al. Multi-year (2013–2016) pm2. 5 wildfire pollution exposure over north america as determined from operational air quality forecasts. *Atmosphere*, 8(9):179, 2017.

[34] Daniel A Jaffe, Susan M O'Neill, Narasimhan K Larkin, Amara L Holder, David L Peterson, Jessica E Halofsky, and Ana G Rappold. Wildfire and prescribed burning impacts on air quality in the united states. *Journal of the Air & Waste Management Association*, 70(6):583–615, 2020.

[35] Erin E McDuffie, Randall V Martin, Joseph V Spadaro, Richard Burnett, Steven J Smith, Patrick O'Rourke, Melanie S Hammer, Aaron van Donkelaar, Liam Bindle, Viral Shah, et al. Source sector and fuel contributions to ambient pm2. 5 and attributable mortality across multiple spatial scales. *Nature communications*, 12(1):1–12, 2021.

[36] Shannon N Koplitz, Christopher G Nolte, George A Pouliot, Jeffrey M Vukovich, and James Beidler. Influence of uncertainties in burned area estimates on modeled wildland fire pm2. 5 and ozone pollution in the contiguous us. *Atmospheric environment*, 191:328–339, 2018.

[37] IN Sokolik, AJ Soja, PJ DeMott, and D Winker. Progress and challenges in quantifying wildfire smoke emissions, their properties, transport, and atmospheric impacts. *Journal of Geophysical Research: Atmospheres*, 124(23):13005–13025, 2019.

[38] M Val Martin, CL Heald, B Ford, AJ Prenni, and C Wiedinmyer. A decadal satellite analysis of the origins and impacts of smoke in colorado. *Atmospheric Chemistry and Physics*, 13(15):7429–7439, 2013.

[39] Crystal D McClure and Daniel A Jaffe. Us particulate matter air quality improves except in wildfire-prone areas. *Proceedings of the National Academy of Sciences*, 115(31):7901–7906, 2018.

[40] Katelyn O'Dell, Bonne Ford, Emily V Fischer, and Jeffrey R Pierce. Contribution of wildland-fire smoke to us pm2. 5 and its influence on recent trends. *Environmental science & technology*, 53(4):1797–1804, 2019.

[41] Taylor Y Wilmot, Derek V Mallia, A Hallar, and John C Lin. Wildfire plumes in the western us are reaching greater heights and injecting more aerosols aloft as wildfire activity intensifies. *Scientific reports*, 12(1):1–14, 2022.

[42] Qian Di, Yan Wang, Antonella Zanobetti, Yun Wang, Petros Koutrakis, Christine Choirat, Francesca Dominici, and Joel D Schwartz. Air pollution and mortality in the medicare population. *New England Journal of Medicine*, 376(26):2513–2522, 2017.

[43] Richard Burnett, Hong Chen, Mieczys law Szyszkowicz, Neal Fann, Bryan Hubbell, C Arden Pope Iii, Joshua S Apte, Michael Brauer, Aaron Cohen, Scott Weichenthal, et al. Global estimates of mortality associated with long-term exposure to outdoor fine particulate matter. *Proceedings of the National Academy of Sciences*, 115(38):9592–9597, 2018.

[44] Yiqun Ma, Emma Zang, Yang Liu, Yuan Lu, Harlan Krumholz, Michelle Bell, and Kai Chen. Wildfire smoke pm2. 5 and mortality in the contiguous united states. *medRxiv*, pages 2023–01, 2023.

[45] Guillermo Rein and Xinyan Huang. Smouldering wildfires in peatlands, forests and the arctic: Challenges and perspectives. *Current Opinion in Environmental Science & Health*, 24:100296, 2021.

[46] Patricia H Gude, Kingsford Jones, Ray Rasker, and Mark C Greenwood. Evidence for the effect of homes on wildfire suppression costs. *International Journal of Wildland Fire*, 22(4):537–548, 2013.

[47] Ruth E Wolf, Suzette A Morman, Geoffrey S Plumlee, Philip L Hageman, and Monique Adams. Release of hexavalent chromium by ash and soils in wildfire-impacted areas. *US Geological Survey Open-File Report*, 1345:22, 2008.

[48] Katie Boaggio, Stephen D LeDuc, R Byron Rice, Parker F Duffney, Kristen M Foley, Amara L Holder, Stephen McDow, and Christopher P Weaver. Beyond particulate matter mass: Heightened levels of lead and other pollutants associated with destructive fire events in california. *Environmental Science & Technology*, 56(20):14272–14283, 2022.

[49] John T Abatzoglou, David S Battisti, A Park Williams, Winslow D Hansen, Brian J Harvey, and Crystal A Kolden. Projected increases in western us forest fire despite growing fuel constraints. *Communications Earth & Environment*, 2(1):1–8, 2021.

[50] Yuanyu Xie, Meiyun Lin, Bertrand Decharme, Christine Delire, Larry W Horowitz, David M Lawrence, Fang Li, and Roland Séférian. Tripling of western us particulate pollution from wildfires in a warming climate. *Proceedings of the National Academy of Sciences*, 119(14):e2111372119, 2022.

[51] Gongbo Chen, Yuming Guo, Xu Yue, Shilu Tong, Antonio Gasparrini, Michelle L Bell, Ben Armstrong, Joel Schwartz, Jouni JK Jaakkola, Antonella Zanobetti, et al. Mortality risk attributable to wildfire-related pm2· 5 pollution: a global time series study in 749 locations. *The Lancet Planetary Health*, 5(9):e579–e587, 2021.

[52] Colleen E Reid, Michael Brauer, Fay H Johnston, Michael Jerrett, John R Balmes, and Catherine T Elliott. Critical review of health impacts of wildfire smoke exposure. *Environmental health perspectives*, 124(9):1334–1343, 2016.

[53] Stephanie M Holm, Mark D Miller, and John R Balmes. Health effects of wildfire smoke in children and public health tools: a narrative review. *Journal of exposure science & environmental epidemiology*, 31(1):1–20, 2021.

[54] Mark Borgschulte, David Molitor, and Eric Zou. Air pollution and the labor market: Evidence from wildfire smoke. *Rev Econ Stat*, 2018.

[55] AF Stein, Roland R Draxler, Glenn D Rolph, Barbara JB Stunder, MD Cohen, and Fong Ngan. Noaa's hysplit atmospheric transport and dispersion modeling system. *Bulletin of the American Meteorological Society*, 96(12):2059–2077, 2015.

[56] Glenn D Rolph, Roland R Draxler, Ariel F Stein, Albion Taylor, Mark G Ruminski, Shobha Kondragunta, Jian Zeng, Ho-Chun Huang, Geoffrey Manikin, Jeffery T McQueen, et al. Description and verification of the noaa smoke forecasting system: the 2007 fire season. *Weather and Forecasting*, 24(2):361–378, 2009.

[57] Tomàs Artés, Duarte Oom, Daniele De Rigo, Tracy Houston Durrant, Pieralberto Maianti, Giorgio Libertà, and Jesús San-Miguel-Ayanz. A global wildfire dataset for the analysis of fire regimes and fire behaviour. *Scientific data*, 6(1):1–11, 2019.

[58] Akli Benali, Ana Russo, Ana CL Sá, Renata MS Pinto, Owen Price, Nikos Koutsias, and José MC Pereira. Determining fire dates and locating ignition points with satellite data. *Remote Sensing*, 8(4):326, 2016.

[59] Ivan Csiszar, Wilfrid Schroeder, Louis Giglio, Evan Ellicott, Krishna P Vadrevu, Christopher O Justice, and Brad Wind. Active fires from the suomi npp visible infrared imaging radiometer suite: Product status and first evaluation results. *Journal of Geophysical Research: Atmospheres*, 119(2):803–816, 2014.

[60] WorldPop. Global 1km population total adjusted to match the corresponding UNPD estimate, 2020.

Supplemental Information

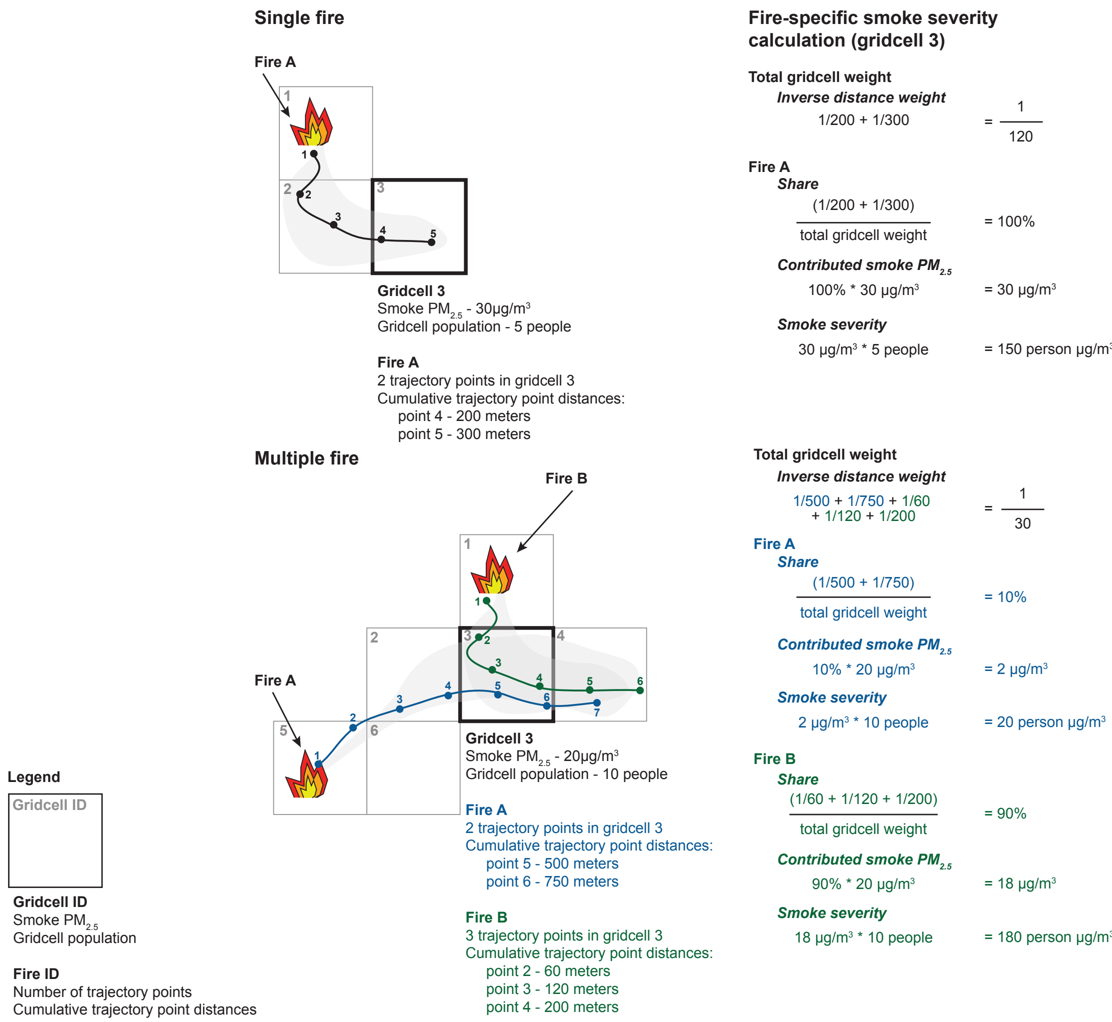

Figure S1: **Smoke severity calculation.** Smoke severity for a specific fire considers the smoke $PM_{2.5}$ contributed by a fire and the total population within affected gridcells. The calculation shown here for gridcell 3 in both the multiple and single fire case represents the smoke severity for each fire in the gridcell. The smoke severity for the fire as a whole aggregates the daily gridcell smoke severity over the duration of the fire. The share of smoke $PM_{2.5}$ contributed by a specific fire is calculated as a function of the number of trajectory points and the cumulative distance of these trajectory points from the initial fire location.

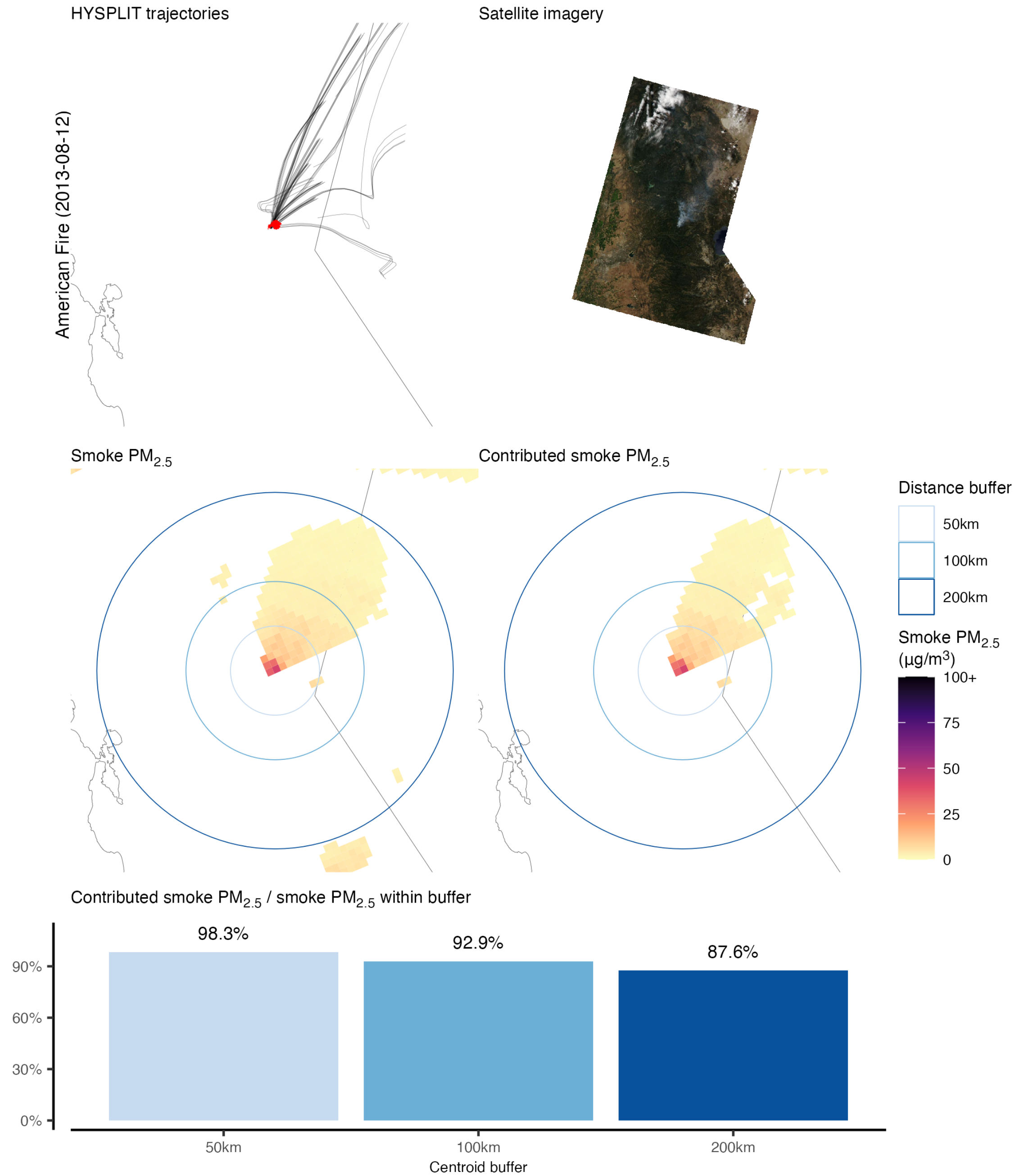

Figure S2: **American Fire contributed smoke $PM_{2.5}$ vs. raw smoke $PM_{2.5}$.** Trajectories, satellite imagery, and smoke $PM_{2.5}$ product all show the smoke generated by the American Fire. The successive concentric buffers around the centroid of the fire calculate the percent of total smoke $PM_{2.5}$ captured by the contributed smoke $PM_{2.5}$ method in this cropped area. The smoke $PM_{2.5}$ in this example appears to come mainly from the American fire with other small plumes noticeable in the "Smoke $PM_{2.5}$ " panel.

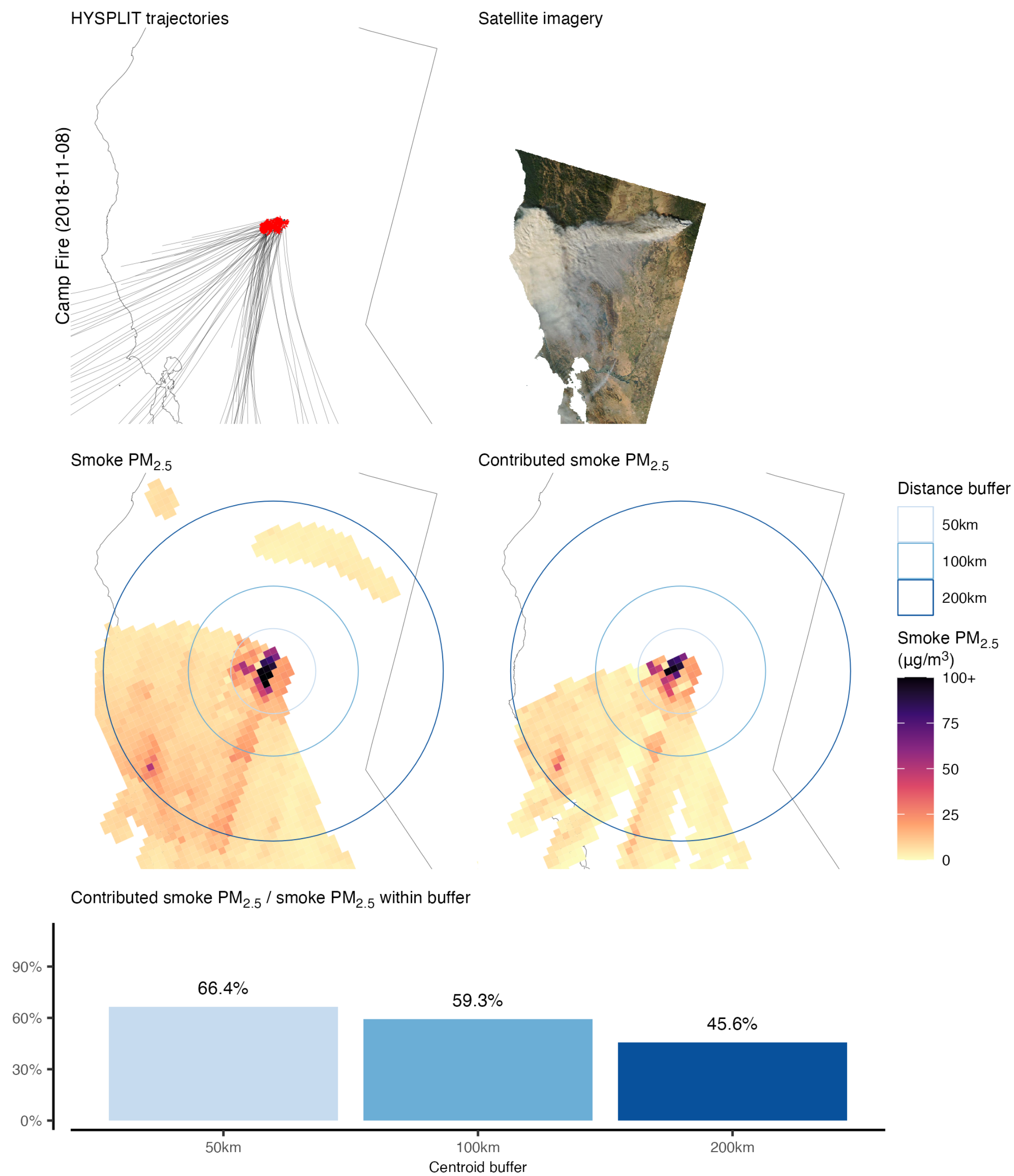

Figure S3: **Camp Fire contributed smoke $PM_{2.5}$ vs. raw smoke $PM_{2.5}$.** The ratio of contributed smoke $PM_{2.5}$ vs. smoke $PM_{2.5}$ is lower for the Camp Fire compared to the American Fire. Other smoke sources are likely producing smoke that is being considered in the total smoke $PM_{2.5}$ calculation. The contributed smoke $PM_{2.5}$ method does not associate these additional plumes to the Camp Fire.

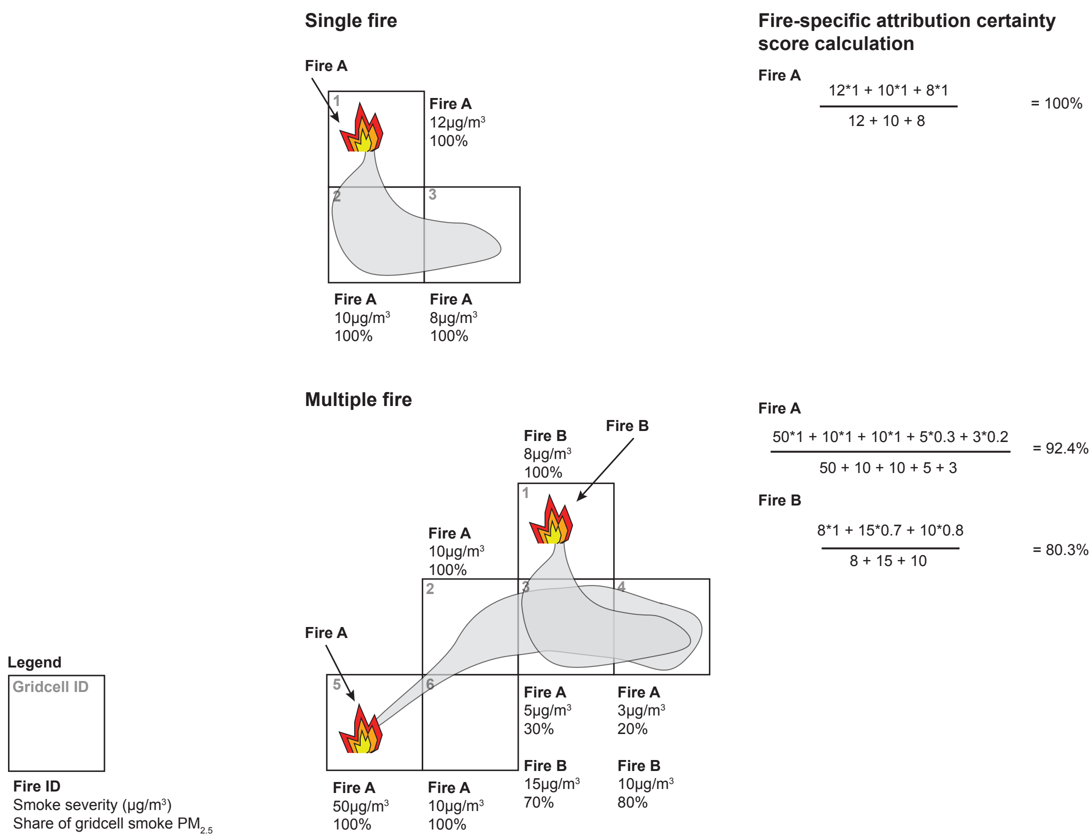

Figure S4: **Attribution certainty score calculation.** The attribution certainty score is a fire-specific estimate of the percent of a given fire's smoke severity that is not coincident with smoke from other fires. Specifically, the measure takes into account the number of trajectory points contributed by a fire, the distance of trajectory points from the source fire, and the smoke $PM_{2.5}$ severity of the fire. A fire with an attribution certainty score of one is a fire whose smoke never overlapped smoke from any other fire. When smoke from multiple fires overlaps, there is less certainty about fire-specific smoke attribution, and the attribution certainty score is lower.

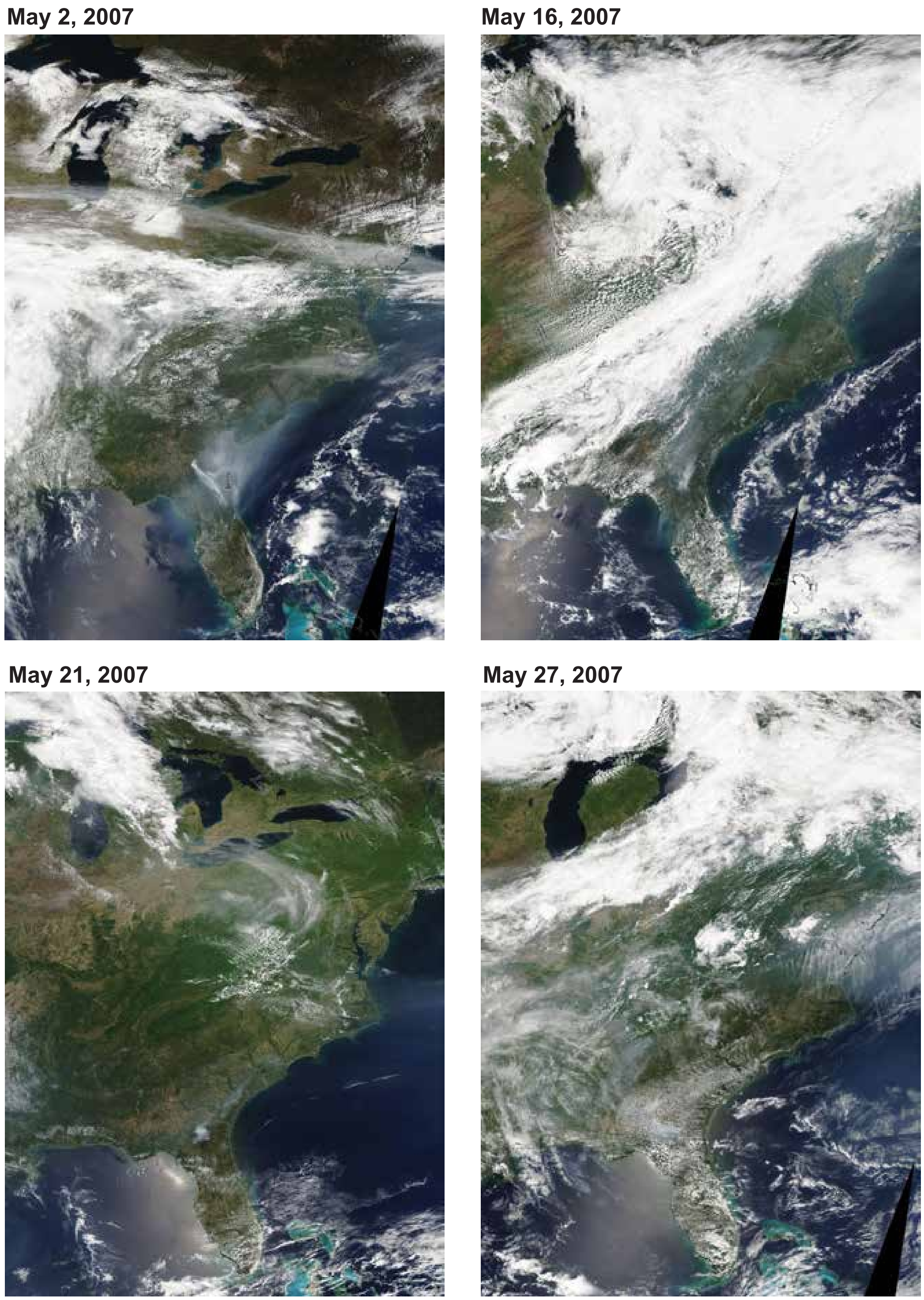

Figure S5: **Bugaboo fire satellite imagery.** The Bugaboo/ Georgia Complex fire burned from April - June 2007 and resulted from several different fires combining together. The smoke $PM_{2.5}$ generated by the fire traveled along much of the Eastern seaboard. The images are from 4 separate days showing the dispersion of smoke. Clouds are also visible in the imagery but are white compared to the gray smoke.

Figure S6: **State-to-state source receptor matrix.** A large proportion of smoke $PM_{2.5}$ affects within state communities although West coast states such as California also contribute a large amount of smoke $PM_{2.5}$ to other states.

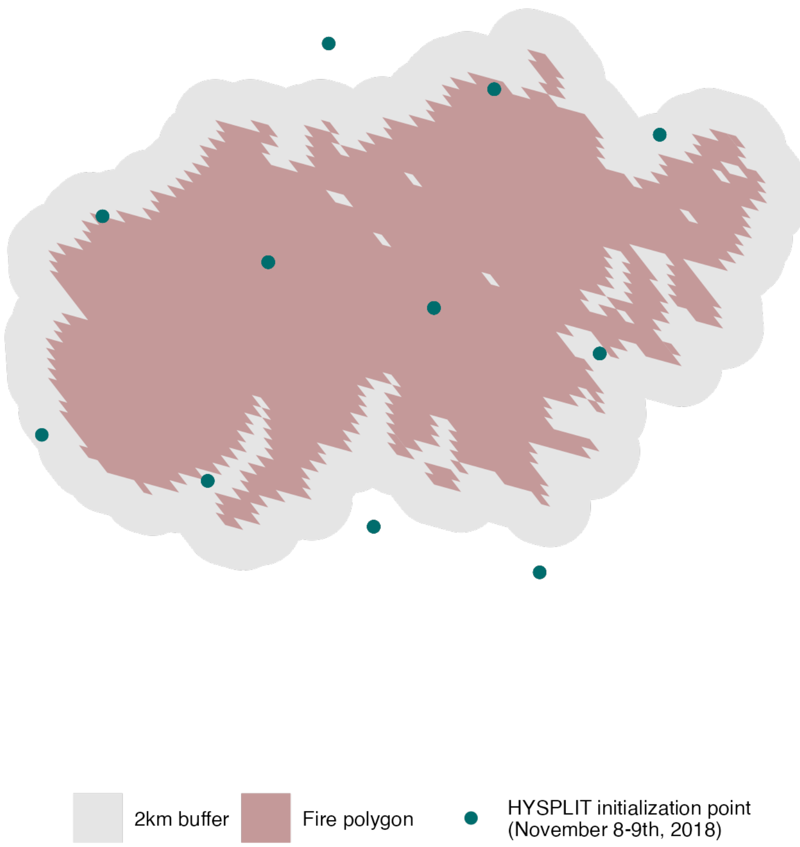

Figure S7: **Camp Fire fire polygon, buffered polygon, and HYSPLIT initialization points.** Smoke producing fire points on November 8-9th show large amounts of overlap with the Camp Fire location, but several HYSPLIT initialization points fall outside of the fire polygon. The rectangular grid of HYSPLIT initialization points suggests that the points were identified by satellite thermal sensors, which may have limited spatial resolution and cause points to fall outside the 2km buffer around fire polygons.

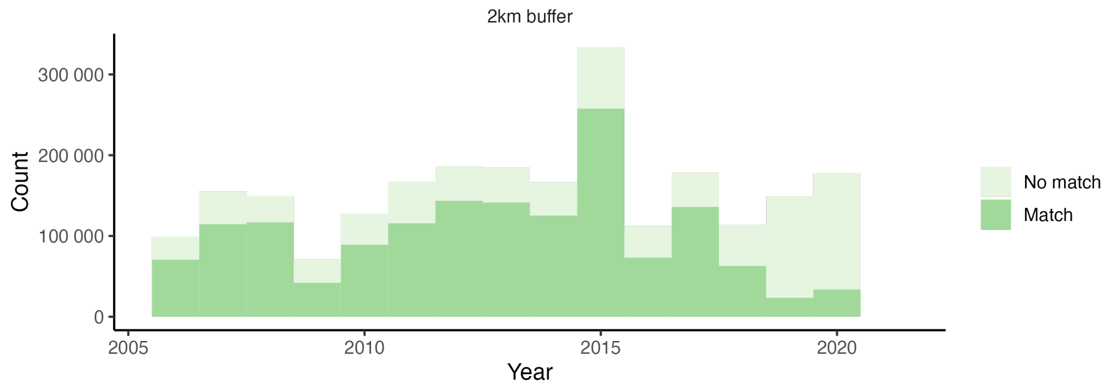

Figure S8: **Yearly distribution of matched vs. unmatched HYSPLIT points.** The trajectories used to distribute smoke $PM_{2.5}$ were generated from analyst identified smoke generating fire points (Method). Over time, different satellite sensors were used to identify fire hotspots with higher resolution satellites introduced around 2016 potentially leading to a greater number of detected thermal anomalies.

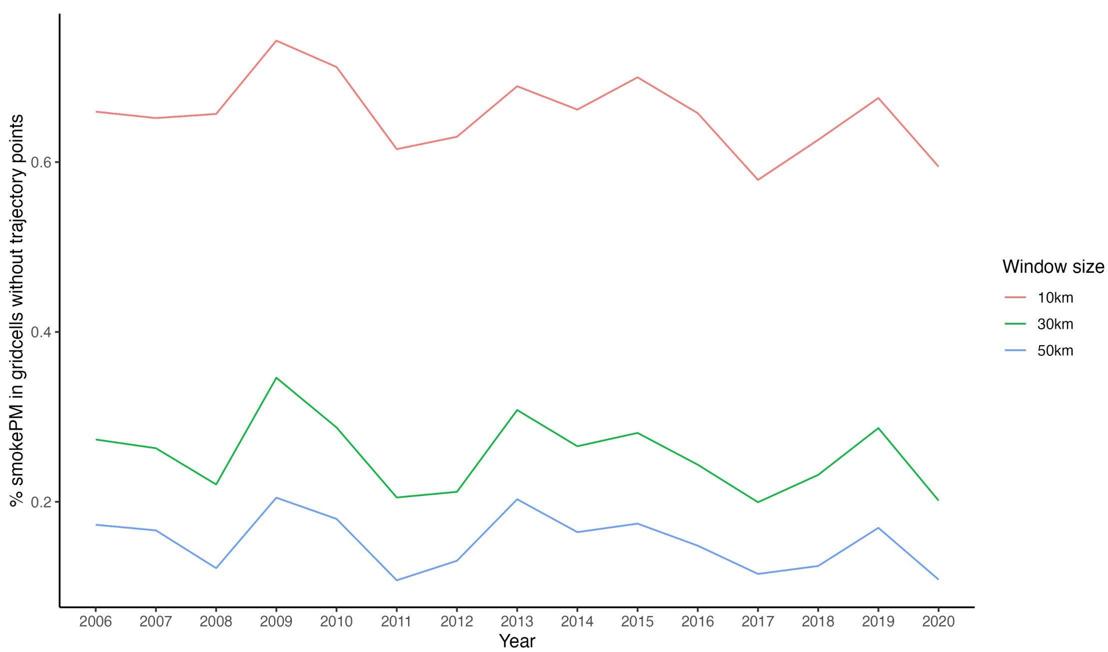

Figure S9: **Comparison of different window sizes to aggregate trajectory points.** The window sizes compare the amount of smoke $PM_{2.5}$ that remains after aggregating neighboring gridcells that may also be affected by smoke. The 10km window does not aggregate neighboring gridcells and only links smoke $PM_{2.5}$ based on the gridcells that intersected with trajectory points. This approach results in the largest amount of unaccounted for smoke $PM_{2.5}$ because smoke is likely to disperse over space away from the path of an average air parcel. Increasing the window size of aggregated neighbors reduces the amount of unaccounted for smoke $PM_{2.5}$.

Table S1: Top 20 fires ranked by population smoke severity

	Fire name	Year	State	Attribution certainty score	Days elapsed	Population smoke $PM_{2.5}$ (billion person $\mu g/m^3$)	Average smoke $PM_{2.5}$ ($\mu g/m^3$)
1	Bugaboo Fire	2007	GA & FL	0.89	54	8.21	13.20
2	August Complex Fire	2020	CA	0.52	71	4.98	5.85
3	Dolan Fire	2020	CA	0.58	42	3.25	4.41
4	Bobcat Fire	2020	CA	0.50	29	3.05	4.54
5	Camp Fire	2018	CA	0.61	17	2.68	13.45
6	Creek Fire	2020	CA	0.43	45	2.45	5.22
7	Ranch Fire (Mendocino Complex)	2018	CA	0.72	51	2.36	5.23
8	Santiam Fire	2020	OR	0.28	49	2.14	4.85
9	Claremont Fire (North Complex)	2020	CA	0.49	57	2.07	4.36
10	SCU Lightning Complex Fire	2020	CA	0.57	28	1.97	5.12
11	Castle Fire (SQF Complex)	2020	CA	0.43	57	1.89	4.08
12	Holiday Farm Fire	2020	OR	0.36	18	1.58	6.63
13	Wallow Fire	2011	AZ	0.82	32	1.51	4.27
14	Hennesey Fire	2020	CA	0.50	25	1.31	4.26
15	Basin Complex Fire	2008	CA	0.73	49	1.28	1.62
16	Archie Creek Fire	2020	OR	0.32	19	1.21	4.50
17	Riverside Fire	2020	OR	0.27	18	1.18	4.87
18	El Dorado Fire	2020	CA	0.43	26	1.10	3.40
19	Glass Fire	2020	CA	0.54	15	1.08	3.80
20	Klondike Fire	2018	OR	0.57	77	1.06	3.08